Chapter 6

Shear locking

In the preceding chapter, we saw a Ritz approximation of the Timoshenko beam problem and noted that it was necessary to ensure a certain consistent relationship between the trial functions to obtain accurate results. We shall now take up the finite element representation of this problem, which is essentially a piecewise Ritz approximation. Our conclusions from the preceding chapter would therefore apply to this as well.

6.1 The linear Timoshenko beam element

An element based on elementary theory needs two nodes with 2 degrees of freedom at each node, the transverse deflection w and slope dw/dx and uses cubic interpolation functions to meet the C^1 continuity requirements of this theory (Fig. 6.1). A similar two-noded beam element based on the shear flexible Timoshenko beam theory will need only C^0 continuity and can be based on simple linear interpolations. It was therefore very attractive for general purpose applications. However, the element was beset with problems, as we shall presently see.

6.1.1 The conventional formulation of the linear beam element

The strain energy of a Timoshenko beam element of length $2l$ can be written as the sum of its bending and shear components as,

$$\int \left(1/2\, EI\, \chi^T\ \chi + 1/2\, kGA\ \gamma^T \gamma \right) dx \tag{6.1}$$

where

$$\chi = \theta_{,x} \tag{6.2a}$$

$$\gamma = \theta - w_{,x} \tag{6.2b}$$

In Equations (6.2a) and (6.2b), w is the transverse displacement and θ the section rotation. E and G are the Young's and shear moduli and the shear correction factor used in Timoshenko's theory. I and A are the moment of inertia and the area of cross-section, respectively.

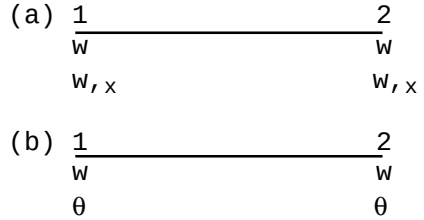

Fig. 6.1 (a) Classical thin beam and (b) Timoshenko beam elements.

In the conventional procedure, linear interpolations are chosen for the displacement field variables as,

$$N_1 = (1-\xi)/2 \qquad (6.3a)$$

$$N_2 = (1+\xi)/2 \qquad (6.3b)$$

where the dimensionless coordinate $\xi = x/l$ varies from -1 to +1 for an element of length $2l$. This ensures that the element is capable of strain free rigid body motion and can recover a constant state of strain (*completeness* requirement) and that the displacements are continuous within the element and across the element boundaries (*continuity* requirement). We can compute the bending and shear strains directly from these interpolations using the strain gradient operators given in Equations (6.2a) and (6.2b). These are then introduced into the strain energy computation in Equation (6.1), and the element stiffness matrix is calculated in an analytically or numerically exact (a *2* point Gauss Legendre integration rule) way.

For the beam element shown in Fig. 6.1, for a length h the stiffness matrix can be split into two parts, a bending related part and a shear related part, as,

$$k_b = EI/h \begin{bmatrix} 0 & 0 & 0 & 0 \\ 0 & 1 & 0 & -1 \\ 0 & 0 & 0 & 0 \\ 0 & -1 & 0 & 1 \end{bmatrix} \quad k_s = kGt/h \begin{bmatrix} 1 & h/2 & -1 & h/2 \\ h/2 & h^2/3 & -h/2 & h^2/6 \\ -1 & -h/2 & 1 & -h/2 \\ h/2 & h^2/6 & -h/2 & h^2/3 \end{bmatrix}$$

We shall now model a cantilever beam under a tip load using this element, considering the case of a "thin" beam with *E=1000, G=37500000, t=1, L=4,* using a fictitiously large value of *G* to simulate the "thin" beam condition. Table 6.1 shows that the normalized tip displacements are dramatically in error. In fact with a classical beam element model, exact answers would have been obtained with one element for this case. We can carefully examine Table 6.1 to see the trend as the number of elements is increased. The tip deflections obtained, which are several orders of magnitude lower than the correct answer, are directly related to the square of the number of elements used for the idealization. In other words, the discretization process has introduced an error so large that the resulting answer has a stiffness related to the inverse of N^2. This is clearly unrelated to the physics of the Timoshenko beam and also not the usual sort of discretization errors encountered in the finite element method. It is this very phenomenon that is known as **shear locking**.

Table 6.1 - Normalized tip deflections

No. of elements	*"Thin" beam*
1	0.200×10^{-5}
2	0.800×10^{-5}
4	0.320×10^{-4}
8	0.128×10^{-3}
16	0.512×10^{-3}

The error in each element must be related to the element length, and therefore when a beam of overall length L is divided into N elements of equal length h, the additional stiffening introduced in each element due to shear locking is seen to be proportional to h^2. In fact, numerical experiments showed that the locking stiffness progresses without limit as the element depth t decreases. Thus, we now have to look for a mechanism that can explain how this spurious stiffness of $(h/t)^2$ can be accounted for by considering the mathematics of the discretization process.

The magic formula proposed to overcome this locking is the reduced integration method. The bending component of the strain energy of a Timoshenko beam element of length $2l$ shown in Equation (6.1) is integrated with a one-point Gaussian rule as this is the minimum order of integration required for exact evaluation of this strain energy. However, a mathematically exact evaluation of the shear strain energy will demand a two-point Gaussian integration rule. It is this rule that resulted in the shear stiffness matrix of rank two that locked. An experiment with a one-point integration of the shear strain energy component causes the shear related stiffness matrix to change as shown below. The performance of this element was extremely good, showing no signs of locking at all (see Table 4.1 for a typical convergence trend with this element).

$$k_b = EI/h \begin{bmatrix} 0 & 0 & 0 & 0 \\ 0 & 1 & 0 & -1 \\ 0 & 0 & 0 & 0 \\ 0 & -1 & 0 & 1 \end{bmatrix} \qquad k_s = kGt/h \begin{bmatrix} 1 & h/2 & -1 & h/2 \\ h/2 & h^2/4 & -h/2 & h^2/4 \\ -1 & -h/2 & 1 & -h/2 \\ h/2 & h^2/4 & -h/2 & h^2/4 \end{bmatrix}$$

6.1.2 The field-consistency paradigm

It is clear from the formulation of the linear Timoshenko beam element using exact integration (we shall call it the *field-inconsistent* element) that ensuring the *completeness* and *continuity* conditions are not enough in some problems. We shall propose a requirement for a *consistent* interpolation of the constrained strain fields as the necessary paradigm to make our understanding of the phenomena complete.

If we start with linear trial functions for w and θ, as we had done in Equation 6.3 above, we can associate two generalized displacement constants with each of the interpolations in the following manner

$$w = a_0 + a_1 \ (x/l) \tag{6.4a}$$

$$\theta = b_0 + b_1 \ (x/l) \tag{6.4b}$$

We can relate such constants to the field-variables obtaining in this element in a discretized sense; thus, $a_1/l = w_{,x}$ at $x=0$, $b_0 = \theta$ and $b_1/l = \theta_{,x}$ at $x=0$. This denotation would become useful when we try to explain how the discretization process can alter the infinitesimal description of the problem if the strain fields are not consistently defined.

If the strain-fields are now derived from the displacement fields given in Equation (6.4), we get

$$\chi = (b_1/l) \tag{6.5a}$$
$$\gamma = (b_0 - a_1/l) + b_1\,(x/l) \tag{6.5b}$$

An exact evaluation of the strain energies for an element of length $h=2l$ will now yield the bending and shear strain energy as

$$U_B = 1/2\ (EI)\ (2l)\ \{(b_1/l)\}^2 \tag{6.6a}$$
$$U_S = 1/2\,(kGA)\ (2l)\ \left\{(b_0 - a_1/l)^2 + 1/3\ b_1^2\right\} \tag{6.6b}$$

It is possible to see from this that in the constraining physical limit of a very thin beam modeled by elements of length $2l$ and depth t, the shear strain energy in Equation (6.6b) must vanish. An examination of the conditions produced by these requirements shows that the following constraints would emerge in such a limit

$$b_0 - a_1/l \to 0 \tag{6.7a}$$
$$b_1 \to 0 \tag{6.7b}$$

In the new terminology that we had cursorily introduced in Section 5.4, constraint (6.7a) is field-consistent as it contains constants from both the contributing displacement interpolations relevant to the description of the shear strain field. These constraints can then accommodate the true Kirchhoff constraints in a physically meaningful way, i.e. in an infinitesimal sense, this is equal to the condition $(\theta\text{-}w_{,x}) \to 0$ at the element centroid. In direct contrast, constraint (6.7b) contains only a term from the section rotation θ. A constraint imposed on this will lead to an undesired restriction on θ. In an infinitesimal sense, this is equal to the condition $\theta_{,x} \to 0$ at the element centroid (i.e. no bending is allowed to develop in the element region). This is the `spurious constraint' that leads to shear locking and violent disturbances in the shear force prediction over the element, as we shall see presently.

6.1.3 An error model for the field-consistency paradigm

We must now determine that this field-consistency paradigm leads us to an accurate error prediction. We know that the discretized finite element model will contain an error which can be recognized when digital computations made with these elements are compared with analytical solutions where available. The *consistency* requirement has been offered as the missing paradigm for the error-free formulation of the constrained media problems. We must now devise an operational procedure that will trace the errors due to an inconsistent representation of the constrained strain field and obtain precise *a priori* measures for these. We must then show by actual numerical experiments with the original elements that the errors are as projected by these *a priori* error models. Only such an exercise will complete the scientific validation of the consistency paradigm. Fortunately, a procedure we shall call the functional re-constitution technique makes it possible to do this verification.

6.1.4 Functional re-constitution

We have postulated that the error of shear locking originates from the spurious shear constraint in Equation (6.7b). We must now devise an error model for the case where the inconsistent element is used to model a beam of length L and depth t. The strain energy for such a beam can be set up as,

$$\Pi = \int_0^L \left\{ 1/2\, EI\ \theta_{,x}^2 + 1/2\, kGA\,(\theta - w_{,x})^2 \right\} dx \tag{6.8}$$

If an element of length $2l$ is isolated, the discretization process produces energy for the element of the form given in Equation (6.6). In this equation, the constants, which were introduced due to the discretization process, can be replaced by the continuum (i.e. the infinitesimal) description. Thus, we note that in each element, the constants in Equations (6.6a) and (6.6b) can be traced to the constants in Equations (6.4a) and (6.4b) and can be replaced by the values of the field variations θ, $\theta_{,x}$ and $w_{,x}$ at the centroid of the element. Thus, the strain energy of deformation in an element is,

$$\pi_e = 1/2\,(EI)(2l)(\theta_{,x})^2 + 1/2\,(kGA)(2l)(\theta - w_{,x})^2 + 1/6\,(kGAl)^2\,(\theta_{,x})^2 \tag{6.9}$$

Thus the constants in the discretized strain energy functional have been re-constituted into an equivalent continuum or infinitesimal form. From this re-constituted functional, we can argue that an idealization of a beam region of length $2l$ into a linear displacement type finite element would produce a modified strain energy density within that region of,

$$\bar{\pi}_e = 1/2\left(EI + kGAl^2/3\right)(\theta_{,x})^2 + 1/2\,(kGA)\,(\theta - w_{,x})^2 \tag{6.10}$$

This strain energy density indicates that the original physical system has been altered due to the presence of the inconsistent term in the shear strain field. Thus, we can postulate that a beam of length L modeled by equal elements of length $2l$ will have a re-constituted functional

$$\bar{\Pi} = \int_0^L \left\{ 1/2\left(EI + kGAl^2/3\right)(\theta_{,x})^2 + 1/2\,(kGA)(\theta - w_{,x})^2 \right\} dx \tag{6.11}$$

We now understand that the discretized beam is stiffer in bending (i.e. its flexural rigidity) by the factor $kGAl^2/3EI$. For a thin beam, this can be very large, and produces the additional stiffening effect described as shear locking.

6.1.5 Numerical experiments to verify error prediction

Our functional re-constitution procedure (note that this is an auxiliary procedure, distinct from the direct finite element procedure that yields the stiffness matrix) allows us to critically examine the consistency paradigm. It indicates that an exactly-integrated or field-inconsistent finite element model tends to behave as a shear flexible beam with a much stiffened flexural rigidity I'. This can be related to the original rigidity I of the system by comparing the expressions in Equations (6.8) and (6.11) as,

$$I'/I = 1 + kGAL^2/3EI \tag{6.12}$$

We must now show through a numerical experiment that this estimate for the error, which has been established entirely *a priori*, starting from the consistency paradigm and introducing the functional re-constitution technique, anticipates very accurately, the behavior of a field-inconsistent linearly interpolated shear flexible element in an actual digital computation. Exact solutions are available for the static deflection W of a Timoshenko cantilever beam of length L and depth t under a vertical tip load. If W_{fem} is the result from a numerical experiment involving a finite element digital computation using elements of length $2l$, the additional stiffening can be described by a parameter as,

$$e_{fem} = W/W_{fem} - 1 \tag{6.13}$$

From Equation (6.12), we already have an *a priori* prediction for this factor as,

$$e = I'/I - 1 = kGAl^2/3EI \tag{6.14}$$

We can now re-interpret the results shown in Table 6.1 for the thin beam case. Using Equations (6.13) and (6.14), we can argue *a priori* that the inconsistent element will produce normalized tip deflections $(W_{fem}/W) = 1/(1+e)$. Since $e>>1$, we have

$$W_{fem}/W = \left(N^2/5\right)\times 10^{-5} \tag{6.15}$$

for the thin beam. Table 6.2 shows how the predictions made thus compare with the results obtained from an actual finite element computation using the field-inconsistent element.

This has shown us that the consistency paradigm can be scientifically verified. Traditional procedures such as counting constraint indices, or computing the rank or condition number of the stiffness matrices could offer only a heuristic picture of how and why locking sets in.

It will be instructive to note here that conventional error analysis norms in the finite element method are based on the percentage error or equivalent in some computed value as compared to the theoretically predicted value. We have seen now that the error of shear locking can be exaggerated without limit, as the structural parameter that acts as a penalty multiplier becomes indefinitely

Table 6.2 - Normalized tip deflections for the thin beam (Case 2) computed from fem model and predicted from error model (Equation (6.15)).

N	*Computed (fem)*	*Predicted*
1	0.200×10^{-4}	0.200×10^{-4}
2	0.800×10^{-4}	0.800×10^{-4}
4	0.320×10^{-3}	0.320×10^{-3}
8	0.128×10^{-3}	0.128×10^{-3}
16	0.512×10^{-3}	0.512×10^{-3}

large. The percentage error norms therefore saturate quickly to a value approaching *100%* and do not sensibly reflect the relationship between error and the structural parameter even on a logarithmic plot. A new error norm called the additional stiffening parameter, *e* can be introduced to recognize the manner in which the errors of locking kind can be blown out of proportion by a large variation in the structural parameter. Essentially, this takes into account, the fact that the spurious constraints give rise to a spurious energy term and consequently alters the rigidity of the system being modeled. In many other examples (e.g. Mindlin plates, curved beams etc.) it was seen that the rigidity, I, of the field consistent system and the rigidity, I', of the inconsistent system, were related to the structural parameters in the form, $I'/I = \alpha(l/t)^2$ where l is an element dimension and t is the element thickness. Thus, if w is the deflection of a reference point as predicted by an analytical solution to the theoretical description of the problem and w_{fem} is the fem deflection predicted by a field inconsistent finite element model, we would expect the relationship described by Equation 6.14. A logarithmic plot of the new error norm against the parameter (l/t) will show a quadratic relationship that will continue indefinitely as (l/t) is increased. This was found to be true of the many constrained media problems. By way of illustration of the distinction made

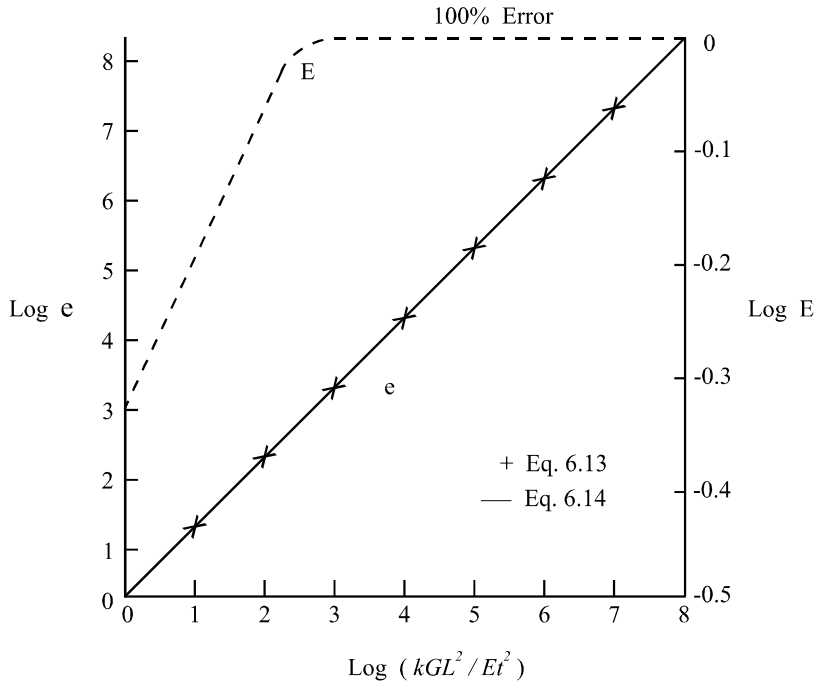

Fig. 6.2 Variation of error norms *e, E* with structural parameter kGL^2/Et^2 for a cantilever beam under tip shear force.

by this definition, we shall anticipate again, the results above. If we represent the conventional error norm in the form $E = (W - W_{fem})/W$, and plot both E and the new error norm e from the results for the same problem using *4 FI* elements against the penalty multiplier $(l/t)^2$ on a logarithmic scale, the dependence is as shown in Fig. 6.2. It can be seen that E saturates quickly to a value approaching *100%* and cannot show meaningfully how the error propagates as the penalty multiplier increases indefinitely. On the other hand, e captures this relationship, very accurately.

6.1.6 Shear Force Oscillations

A feature of inconsistently modeled constrained media problems is the presence of spurious violently oscillating strains and stresses. It was not understood for a very long time that in many cases, stress oscillations originated from the inconsistent constraints. For a cantilever beam under constant bending moment modeled using linear Timoshenko beam elements, the shear force (stresses) displays a saw-tooth pattern (we shall see later that a plane stress model using 4-node elements will also give an identical pattern on the neutral bending surface). We can arrive at a prediction for these oscillations by applying the functional re-constitution technique.

If $\bar{V}$ is the shear force predicted by a field-consistent shear strain field (we shall see soon how the field-consistent element can be designed) and V the shear force obtained from the original shear strain field, we can write from Equation (6.5b),

$$\bar{V} = kGA\,(b_0 - a_1/l) \tag{6.16a}$$

$$V = \bar{V} + kGA\,b_1\,(x/l) \tag{6.16b}$$

We see that V has a linear term that relates directly to the constant that appeared in the spurious constraint, Equation (6.7b). We shall see below from Equation (6.17) that b_1 will not be zero, in fact it is a measure of the bending moment at the centroid of the element. Thus, in a field-inconsistent formulation, this constant will activate a violent linear shear force variation when the shear forces are evaluated directly from the shear strain field given in Equation (6.5b). The oscillation is self-equilibrating and does not contribute to the force equilibrium over the element. However, it contributes a finite energy in Equation (6.9) and in the modeling of very slender beams, this spurious energy is so large as to completely dominate the behavior of the beam and cause a locking effect.

Figure 6.3 shows the shear force oscillations in a typical problem - a straight cantilever beam with a concentrated moment at the tip. One to ten equal length field-inconsistent elements were used and shear forces were computed at the nodes of each element. In each case, only the variation within the element at the fixed end is shown, as the pattern repeats itself in a saw-tooth manner over all other elements. At element mid-nodes, the correct shear force i.e. $V=0$ is reproduced. Over the length of the element, the oscillations are seen to be linear functions corresponding to the $kGA\ b_1\ (x/l)$ term. Also indicated by the solid lines, is the prediction made by the functional re-constitution exercise. We shall explore this now.

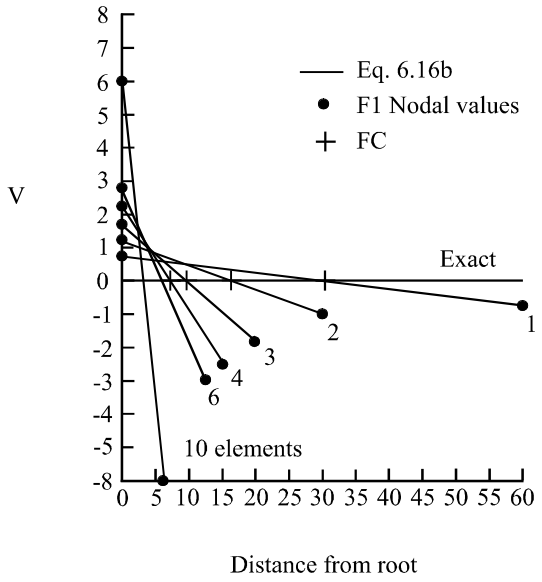

Fig. 6.3 Shear force oscillations in element nearest the root, for N element models of a cantilever of length L = 60.

Consider a straight cantilever beam with a tip shear force Q at the free end. This should produce a linearly varying bending moment M and a constant shear force Q in the beam. An element of length $2l$ at any station on the beam will now respond in the following manner. Since, a linear element is used, only the average of the linearly varying bending moment is expected in each finite element. If the element is field-consistent, the constant b_1 can be associated after accounting for discretization, to relate to the constant bending moment M_0 at the element centroid as,

$$M_0 = EI\, b_1 / l \quad \text{or}$$

$$b_1 = M_0 l / EI \tag{6.17}$$

In a field-inconsistent problem, due to shear locking, it is necessary to consider the modified flexural rigidity I' (see Equation 6.17) that modifies b_1 to b_1', that is,

$$\begin{aligned} b_1' &= M_0 l / EI' \\ &= \{M_0 l / EI(1+e)\} \\ &= b_1 / (1+e) \end{aligned} \tag{6.18}$$

where $e = kGAl^2 / 3EI$.

Thus, in a field-inconsistent formulation, the constant b_1 gets stiffened by the factor e; the constant bending moment M_0 is also underestimated by the

same factor. Also, for a very thin beam where $e>>1$, the centroidal moment M_0 predicted by a field-consistent element diminishes in a t^2 rate for a beam of rectangular cross-section. These observations have been confirmed through digital computation.

The field-consistent element will respond with $\bar{V} = V_0 = Q$ over the entire element length $2l$. The field-inconsistent shear force V from Equations (6.16) and (6.18) can be written for a very thin beam $(e>>1)$ as,

$$V = Q + (3M_0/l)(x/l) \tag{6.19}$$

These are the violent shear force linear oscillations within each element, which originate directly from the field-inconsistency in the shear strain definition.

These oscillations are also seen if field-consistency had been achieved in the element by using reduced integration for the shear strain energy. Unless the shear force is sampled at the element centroid (i.e. Gaussian point, $x/l=0$), these disturbances will be much more violent than in the exactly integrated version.

6.1.7 The consistent formulation of the linear element

We can see that reduced integration ensures that the inconsistent constraint does not appear and so is effective in producing a consistent element, at least in this instance. We must now satisfy ourselves that such a modification did not violate any variational theorem.

The field-consistent element, as we now shall call an element version free of spurious (i.e. inconsistent) constraints, can and has been formulated in various other ways as well. The `trick' is to evaluate the shear strain energy, in this instance, in such a way that only the consistent term will contribute to the shear strain energy. Techniques like addition of bubble modes, hybrid methods etc. can produce the same results, but in all cases, the need for consistency of the constrained strain field must be absolutely met.

We explain now why the use of a trick like the reduced integration technique, or the use of assumed strain methods allows the locking problem to be overcome. It is obvious that it is not possible to reconcile this within the ambit of the minimum total potential principle only, which had been the starting point of the conventional formulation.

We saw in Chapter 2, an excellent example of a situation where it was necessary to proceed to a more general theorem (one of the so-called mixed theorems) to explain why the finite element method computed strain and stress fields in a `best-fit' sense. We can now see that in the case of constrained media problems, the mixed theorem such as the Hu-Washizu or Hellinger-Reissner theorem can play a crucial role in proving that by modifying the minimum total potential based finite element formulation by using an assumed strain field to replace the kinematically derived constrained field, no energy, or work principle or variational norms have been violated.

To eliminate problems such as locking, we look for a consistent constrained strain field to replace the inconsistent kinematically derived strain field in the minimum total potential principle. By closely examining the strain gradient operators, it is possible to identify the order up to which the consistent strain field must be interpolated. In this case, for the linear displacement interpolations, Equations (6.5b), (6.7a) and (6.7b) tell us that the consistent interpolation should be a constant. At this point we shall still not presume what this constant should be, although past experience suggests it is the same constant term seen in Equation (6.7a). Instead, we bring in the Hellinger-Reissner theorem in the following form to see the identity of the consistent strain field clearly. For now, it is sufficient to note that the Hellinger-Reissner theorem is a restricted case of the Hu-Washizu theorem. In this theorem, the functional is stated in the following form,

$$\int \left(-1/2\, EI\, \bar{\chi}^T \bar{\chi} + EI\, \bar{\chi}^T \chi - 1/2\, kGA\, \bar{\gamma}^T \bar{\gamma} + kGA\, \bar{\gamma}^T \gamma \right) dx \tag{6.20}$$

where $\bar{\chi}$ and $\bar{\gamma}$ are the new strain variables introduced into this multi-field principle. Since we have difficulty only with the kinematically derived γ we can have $\bar{\chi} = \chi$ and recommend the use of a $\bar{\gamma}$ which is of consistent order to replace γ. A variation of the functional in Equation (6.20) with respect to the as yet undetermined coefficients in the interpolation for $\bar{\gamma}$ yields

$$\int \delta\bar{\gamma}^T \left(\bar{\gamma} - \gamma \right) dx = 0 \tag{6.21}$$

This orthogonality condition now offers a means to constitute the coefficients of the consistent strain field from the already known coefficients of the kinematically derived strain field. Thus, for γ given by Equation (6.5b), it is possible to show that $\bar{\gamma} = \left(b_0 - \alpha_1 / l \right)$. In this simple instance, the same result is obtained by sampling the shear strain at the centroid, or by the use of one-point Gaussian integration. What is important is that, deriving the consistent strain-field using this orthogonality relation and then using this to compute the corresponding strain energy will yield a field-consistent element which does not violate any of the variational norms, i.e. an exact equivalence to the mixed element exists without having to go through the additional operations in a mixed or hybrid finite element formulation, at least in this simple instance. We say that the variational correctness of the procedure is assured. The substitute strain interpolations derived thus can therefore be easily coded in the form of strain function subroutines and used directly in the displacement type element stiffness derivations.

6.1.8 Some concluding remarks on the linear beam element

So far we have seen the linear beam element as an example to demonstrate the principles involved in the finite element modeling of a constrained media problem. We have been able to demonstrate that a conceptual framework that includes a condition that specifies that the strain fields which are to be constrained must satisfy a *consistency* criterion is able to provide a complete scientific basis for the locking problems encountered in conventional displacement type modeling. We have also shown that a *correctness* criterion (which links the assumed strain variation of the displacement type formulation

to the mixed variational theorems) allows us to determine the consistent strain field interpolation in a unique and mathematically satisfying manner.

It will be useful now to see how these concepts work if a quadratic beam element is to be designed. This is a valuable exercise as later, the quadratic beam element shall be used to examine problems such as encountered in curved beam and shell elements and in quadrilateral plate elements due to non-uniform mapping.

6.2 The quadratic Timoshenko beam element

We shall now very quickly see how the field-consistency rules explain the behavior of a higher order element. We saw in Chapter 5 that the conventional formulation with lowest order interpolation functions led to spurious constraints and a non-singular assembled stiffness matrix, which result in locking. In a higher order formulation, the matrix was singular but the spurious constraints resulted in a system that had a higher rank than was felt to be desirable. This resulted in sub-optimal performance of the approximation. We can now use the quadratic beam element to demonstrate that this is true in finite element approximations as well.

6.2.1 The conventional formulation

Consider a quadratic beam element designed according to conventional principles, i.e. exact integration of all energy terms arising from a minimum total potential principle. As the beam becomes very thin, the element does not lock; in fact it produces reasonably meaningful results. Fig. 6.4 shows a typical comparison between the linear and quadratic beam elements in its application to a simple problem. A uniform cantilever beam of length *1.0 m*, width *0.01 m* and depth *0.01 m* has a vertical tip load of *100 N* applied at the tip. For $E=10^{10}$ N/m^2 and $\mu=0.3$, the engineering theory of beams predicts a tip deflection of $w=4.0$ m. We shall consider three finite element idealizations of this problem - with the linear 2-node field-consistent element considered earlier in this section (2C, on the Figure), the quadratic 3-node field-inconsistent element being discussed now (3I, on the Figure) and the quadratic 3-node field-consistent element which we shall derive later (3C). It is seen that for this simple problem, the 3C element produces exact results, as it is able to simulate the constant shear and linear bending moment variation along the beam length. The 3I and 2C elements show identical convergence trends and behave as if they are exactly alike. The curious aspects that call for further investigation are: the quadratic element (3I) behaves in exactly the same way as the field-consistent linear element (2C), giving exactly the same accuracy for the same number of elements although the system assembled from the former had nearly twice as many nodes. It also produced moment predictions, which were identical, i.e., the quadratic beam element, instead of being able to produce linear-accurate bending moments could now yield only a constant bending moment within each element, as in the field-consistent linear element. Further, there were now quadratic oscillations in the shear force predictions for such an element. Note now that these curious features cannot be explained from the old arguments, which linked locking to the non-singularity or the large rank or the spectral condition number of the stiffness matrix. We shall now proceed to explain these features using the field-consistency paradigm.

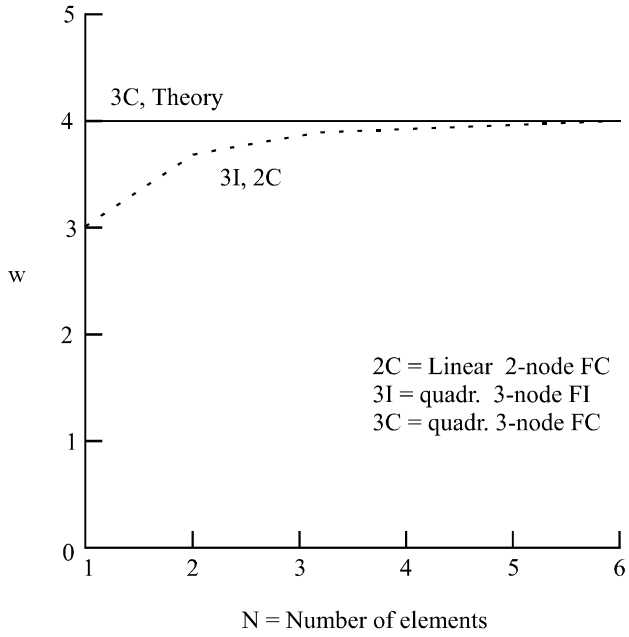

Fig. 6.4 A uniform cantilever beam with tip shear force - convergence trends of linear and quadratic elements.

If quadratic isoparametric functions are used for the field-variables w and θ in the following manner

$$w = a_0 + a_1 (x/l) + a_2 (x/l)^2$$
$$\theta = b_0 + b_1 (x/l) + b_2 (x/l)^2$$

the shear strain interpolation will be,

$$\gamma = (b_0 + b_2/3 - a_1/l) + (b_1 - 2a_2/l)\xi - b_2/3\left(1 - 3\xi^2\right) \tag{6.22}$$

Again, we emphasize the usefulness of expanding the strain field in terms of the Legendre polynomials. When the strain energies are integrated, because of the orthogonal nature of the Legendre polynomials the discretized energy expression becomes the sum of the squares of the coefficients multiplying the Legendre polynomials. Indeed, the strain energy due to transverse shear strain is,

$$U_s = 1/2\,(kGA)(2l)\,\left\{(b_0 + b_2/3 - a_1/l)^2 + 1/3\,(b_1 - 2a_2/l)^2 + 4b_2^2/45\right\} \tag{6.23}$$

Therefore, when we introduce the penalty limit condition that for a thin beam the shear strain energies must vanish, we can argue that the coefficients of the strain field expanded in terms of the Legendre polynomials must vanish separately. In this case, three constraints emerge:

$$(b_0 + b_2/3 - a_1/l) \to 0 \tag{6.24a}$$

$$(b_1 - 2a_2/l) \to 0 \qquad (6.24b)$$

$$b_2 \to 0 \qquad (6.24c)$$

Equations (6.24a) and (6.24b) represent constraints having contributions from the field interpolations for both w and θ. They can therefore reproduce, in a consistent manner, true constraints that reflect a physically meaningful imposition of the thin beam Kirchhoff constraint. This is therefore the *field-consistent* part of the shear strain interpolation.

Equation (6.24c) however contains a constant only from the interpolation for θ. This constraint, when enforced, is an unnecessary restriction on the freedom of the interpolation for θ, constraining it in fact to behave only as a linear interpolation as the constraint implies that $\theta_{,xx} \to 0$ in a discretized sense over each beam element region. The spurious energy implied by such a constraint does not contribute directly to the discretized bending energy, unlike the linear beam element seen earlier. Therefore, field-inconsistency in this element would not cause the element to lock. However, it will diminish the rate of convergence of the element and would induce disturbances in the form of violent quadratic oscillations in the shear force predictions, as we shall see in the next section.

6.2.2 Functional reconstitution

We can use the functional re-constitution technique to see how the inconsistent terms in the shear strain interpolation alter the description of the physics of the original problem (we shall skip most of the details, as the material is available in greater detail in Ref. 6.1).

The b_2 term that appears in the bending energy also makes an appearance in the shear strain energy, reflecting its origin through the spurious constraint. We can argue that this accounts for the poor behavior of the field-inconsistent quadratic beam element (the 3I of Fig. 6.4). Ref. 6.1 derives the effect more precisely, demonstrating that the following features can be fully accounted for:

i) the displacement predictions of the 3I element are identical to that made by the 2C element on an element by element basis although it has an additional mid-node and has been provided with the more accurate quadratic interpolation functions.
ii) the 3I element can predict only a constant moment within each element, exactly as the 2C element does.
iii) there are quadratic oscillations in the shear force field within each element.

We have already discussed earlier that the 3I element (the field-inconsistent 3-noded quadratic) converges in exactly the same manner as the 2C element (the field-consistent linear). This has been explained by showing using the functional re-constitution technique, that the b_2 term, which describes the linear variation in the bending strain and bending moment interpolation, is "locked" to a vanishingly small value. The 3I element then effectively behaves as a 2C element in being able to simulate only a constant bending-moment in each region of a beam, which it replaces.

6.2.3 The consistent formulation of the quadratic element

As in the linear element earlier, the field-consistent element (3C) can be formulated in various ways. Reduced integration of the shear strain energy using a 2-point Gauss-Legendre formula was the most popular method of deriving the element so far. Let us now derive this element using the `assumed' strain approach. We use the inverted commas to denote that the strain is not assumed in an arbitrary fashion but is actually uniquely determined by the consistency and the variational correctness requirements. The re-constitution of the field is to be done in a variationally correct way, i.e. we are required to replace γ in Equation (6.22) which had been derived from the kinematically admissible displacement field interpolations using the strain-displacement operators with an `assumed' strain field $\bar{\gamma}$ which contains terms only upto and including the linear Legendre polynomial in keeping with the consistency requirement. Let us write this in the form

$$\bar{\gamma} = c_0 + c_1 \xi \tag{6.25}$$

The orthogonality condition in Equation (6.21) dictates how $\bar{\gamma}$ should replace γ over the length of the element. This determines how c_0 and c_1 should be constituted from b_0, b_1 and b_2. Fortunately, the orthogonal nature of the Legendre polynomials allows this to be done for this example in a very trivial fashion. The quadratic Legendre polynomial and its coefficient are simply truncated and $c_0=b_0$ and $c_1=b_1$ represent the variationally correct field-consistent `assumed' strain field. The use of such an interpolation subsequently in the integration of the shear strain energy is identical to the use of reduced integration or the use of a hybrid assumed strain approach. In a hybrid assumed strain approach, such a consistent re-constitution is automatically implied in the choice of assumed strain functions and the operations leading to the derivation of the flexibility matrix and its inversion leading to the final stiffness matrix.

6.3 The Mindlin plate elements

A very large part of structural analysis deals with the estimation of stresses and displacements in thin flexible structures under lateral loads using what is called plate theory. Thus, plate elements are the most commonly used elements in general purpose structural analysis. At first, most General Purpose Packages (GPPs) for structural analysis used plate elements based on what are called the C^1 theories. Such theories had difficulties and limitations and a1so attention turned to what are called the C^0 theories.

The Mindlin plate theory [6.2] is now the most commonly used basis for the development of plate elements, especially as they can cover applications to moderately thick and laminated plate and shell constructions. It has been estimated that in large scale production runs using finite element packages, the simple four-node quadrilateral plate element (the QUAD4 element) may account for as much as *80%* of all usage. It is therefore important to understand that the evolution of the current generation of QUAD4 elements from those of yester-year, over a span of nearly three decades was made difficult by the presence of shear locking. We shall now see how this takes place.

The history behind the discovery of *shear locking* in plate elements is quite interesting. It was first recognized when an attempt was made to represent the behavior of shells using what is called the degenerate shell approach [6.3]. In this the shell behavior is modeled directly after a slight modification of the 3D equations and shell geometry and domain are represented by a 3D brick element but its degrees of freedom are condensed to three displacements and two section rotations at each node. Unlike classical plate or shell theory, the transverse shear strain and its energy is therefore accounted for in this formulation. Such an approach was therefore equivalent to a Mindlin theory formulation. These elements behaved very poorly in representing even the trivial example of a plate in bending and the errors progressed without limit, as the plates became thinner. The difficulty was attributed to shear locking. This is in fact the two-dimensional manifestation of the same problem that we encountered for the Timoshenko beam element; ironically it was noticed first in the degenerate shell element and was only later related to the problems in designing Timoshenko beam and Mindlin plate elements [6.4]. The remedy proposed at once was the reduced integration of the shear strain energy [6.5,6.6]. This was only partially successful and many issues remained unresolved. Some of these were,

i) the 2×2 rule failed to remove shear locking in the 8-node serendipity plate element,
ii) the 2×2 rule in the 9-node Lagrangian element removed locking but introduced zero energy modes,
iii) the selective 2×3 and 3×2 rule for the transverse shear strain energies from γ_{xz} and γ_{yz} recommended for a 8-node element also failed to remove shear locking,
iv) the same selective 2×3 and 3×2 rule when applied to a 9-noded element is optimal for a rectangular form of the element but not when the element was distorted into a general quadrilateral form,
v) even after reduced integration of the shear energy terms, the degenerate shell elements performed poorly when trying to represent the bending of curved shells, due to an additional factor, identified as **membrane locking** [6.7], originating now from the need for consistency of the membrane strain interpolations. We shall consider the membrane-locking phenomenon in another section.

We shall confine our study now to plate elements without going into the complexities of the curved shell elements.

In Kirchhoff-Love thin plate theory, the deformation is completely described by the transverse displacement w of the mid-surface. In such a description, the transverse shear deformation is ignored. To account for transverse shear effects, it is necessary to introduce additional degrees of freedom. We shall now consider Mindlin's approximations, which have permitted such an improved description of plate behavior. The degenerate shell elements that we discussed briefly at the beginning of this section can be considered to correspond to a Mindlin type representation of the transverse shear effects.

In Mindlin's theory [6.2], deformation is described by three quantities, the section rotations θ_x and θ_y (i.e. rotations of lines normal to the midsurface of the undeformed plate) and the mid-surface deflection w. The bending strains are now derived from the section rotations and do not cause any

difficulty when a finite element model is made. The shear strains are now computed as the difference between the section rotations and the slopes of the neutral surfaces, thus,

$$\gamma_{xz} = \theta_x - w_{,x}$$
$$\gamma_{yz} = \theta_y - w_{,y} \qquad (6.26)$$

The stiffness matrix of a Mindlin plate element will now have terms from the bending strain energy and the shear strain energy. It is the inconsistent representation of the latter that causes shear locking.

6.3.1 The 4-node plate element

The 4-node bi-linear element is the simplest element based on Mindlin theory that could be devised. We shall first investigate the rectangular form of the element [6.4] as it is in this configuration that the consistency requirements can be easily understood and enforced. In fact, an optimum integration rule can be found which ensures consistency if the element is rectangular. It was established in Ref. 6.4 that an exactly integrated Mindlin plate element would lock even in its rectangular form. Locking was seen to vanish for the rectangular element if the bending energy was computed with a *2×2* Gaussian integration rule while a reduced *1*-point rule was used for the shear strain energy. This rectangular element behaved very well if the plate was thin but the results deteriorated as the plate became thicker. Also, after distortion to a quadrilateral form, locking re-appeared. A spectral analysis of the element stiffness matrix revealed a rank deficiency - there were two zero energy mechanisms in addition to the usual three rigid body modes required for such an element. It was the formation of these mechanisms that led to the deterioration of element performance if the plate was too thick or if it was very loosely constrained. It was not clear why the quadrilateral form locked even after reduced integration. We can now demonstrate from our consistency view-point why the *1*-point integration of the shear strain energy is inadequate to retain all the true Kirchhoff constraints in a rectangular thin plate element. However, we shall postpone the discussion on why such a strategy cannot preserve consistency if the element was distorted to a later section.

Following Ref. [6.4], the strain energy for an isotropic, linear elastic plate element according to Mindlin theory can be constituted from its bending and shear energies as,

$$U = U_B + U_S$$

$$= \frac{Et^2}{24(1-\nu^2)} \left\{ \int\int \left[\theta_{x,x}^2 + \theta_{y,y}^2 + 2\nu\, \theta_{x,x}\, \theta_{y,y} \right.\right.$$

$$\left.\left. + (1-\nu)/2\, (\theta_{x,y} + \theta_{y,x})^2 \right] dx\, dy \right. \qquad (6.27)$$

$$\left. + \frac{6k(1-\nu)}{t^2} \int\int \left[(\theta_x - w_{,x})^2 + (\theta_y - w_{,y})^2 \right] dx\, dy \right\}$$

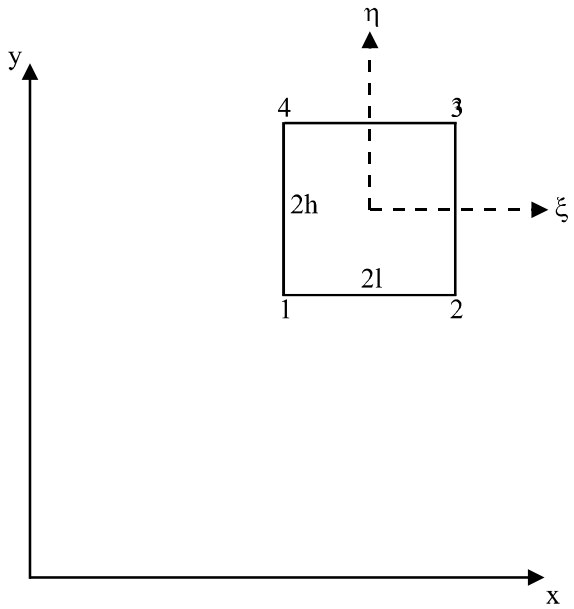

Fig. 6.5 Cartesian and natural coordinate system for a four-node rectangular plate element.

where x, y are Cartesian co-ordinates (see Fig. 6.5), w is the transverse displacement, θ_x and θ_y are the section rotations, E is the Young's modulus, ν is the Poisson's ratio, k is the shear correction factor and t is the plate thickness. The factor k is introduced to compensate for the error in approximating the shear strain as a constant over the thickness direction of a Mindlin plate.

Let us now examine the field-consistency requirements for one of the shear strains, γ_{xz}, in the Cartesian system. The admissible displacement field interpolations required for a 4-node element can be written in terms of the Cartesian co-ordinates itself as,

$$w = a_0 + a_1 x + a_2 y + a_3 xy \tag{6.28a}$$

$$\theta = b_0 + b_1 x + b_2 y + b_3 xy \tag{6.28b}$$

The shear strain field derived from these kinematically admissible shape functions is,

$$\gamma_{xz} = (b_0 - a_1) + (b_2 - a_3) y + b_1 x + b_3 xy \tag{6.29}$$

As the plate thickness is reduced to zero, the shear strains must vanish. The discretized constraints that are seen, to be enforced as $\gamma_{xz} \to 0$ in Equation (6.29) are,

$$b_0 - a_1 \to 0 \tag{6.30a}$$

$$b_2 - a_3 \to 0 \tag{6.30b}$$

$$b_1 \to 0 \tag{6.30c}$$

$$b_3 \to 0 \tag{6.30d}$$

The constraints shown in Equations (6.30a) and (6.30b) are physically meaningful and represent the Kirchhoff condition in a discretized form. Constraints (6.30c) and (6.30d) are the cause for concern here - these are the spurious or `inconsistent' constraints which lead to shear locking. Thus, in a rectangular element, the requirement for consistency of the interpolations for the shear strains in the Cartesian co-ordinate system is easily recognized as the polynomials use only Cartesian co-ordinates. Let us now try to derive the optimal element and also understand why the simple *1*-point strategy of Ref. 6.4 led to zero energy mechanisms.

It is clear from Equations (6.29) and (6.30) that the terms b_1x and b_3xy are the inconsistent terms which will contribute to locking in the form of spurious constraints. Let us now look for optimal integration strategies for removing shear locking without introducing any zero energy mechanisms. We shall consider first, the part of the shear strain energy contributed by γ_{xz}. We must integrate exactly, terms such as $(b_0\text{-}a_1)$, $(b_2\text{-}a_3)y$, b_1x, and b_3xy. We now identify terms such as $(b_0\text{-}a_1)$, $(b_2\text{-}a_3)$, b_1, and b_3 as being equivalent to the quantities $(\theta_x\text{-}w_{,x})_0$, $(\theta_x\text{-}w_{,x})_{,y0}$, $(\theta_{x,x})_0$, and $(\theta_{x,xy})_0$ where the subscript '*0*' denotes the values at the centroid of the element (for simplicity, we let the centroid of the element lie at the origin of the Cartesian co-ordinate system).

An exact integration, that is a *2×2* Gaussian integration of the shear strain energy leads to

$$\int\int \gamma_{xz}^2 dx\, dy = 4lh\left[(\theta_x - w_{,x})_0^2 + h^2/3\,(\theta_x - w_{,x})^2{}_{,y0} + l^2/3\,(\theta_{x,x})_0^2 + h^2l^2/9\,(\theta_{x,xy})_0^2\right] \qquad (6.31)$$

In the penalty limit of a thin plate, these four quantities act as constraints. The first two reproduce the true Kirchhoff constraints and the remaining two act as spurious constraints that cause shear locking by enforcing $\theta_{x,x}\rightarrow 0$ and $\theta_{x,xy}\rightarrow 0$ in the element.

If a *1×2* Gaussian integration is used, we have,

$$\int\int \gamma_{xz}^2 dx\, dy = 4lh\left[(\theta_x - w_{,x})_0^2 + h^2/3\,(\theta_x - w_{,x})^2{}_{,y0}\right] \qquad (6.32)$$

Thus, only the true constraints are retained and all spurious constraints are removed. This strategy can also be seen to be variationally correct in this case; we shall see later that in a quadrilateral case, it is not possible to ensure variational correctness exactly. By a very similar argument, we can show that the part of the shear strain energy from γ_{yz} will require a *2×1* Gaussian integration rule. This element would be the optimal rectangular bi-linear Mindlin plate element.

Let us now look at the *1*-point integration strategy used in Ref. 6.4. This will give shear energy terms such as,

$$\int\int \gamma_{xz}^2\, dx\, dy = 4lh\left[(\theta_x - w_{,x})_0^2\right] \qquad (6.33)$$

We have now only one true constraint each for the shear energy from γ_{xz} and γ_{yz} respectively while the other Kirchhoff constraints $(\theta_x - w_{,x})_{,y0} \rightarrow 0$ and $(\theta_y - w_{,y})_{,x0} \rightarrow 0$ are lost. This introduces two zero energy modes and accounts for the consequent deterioration in performance of the element when the plates are thick or are very loosely constrained, as shown in Ref. 6.4.

We have seen now that it is a very simple procedure to re-constitute field-consistent assumed strain fields from the kinematically derived fields such as shown in Equation (6.29) so that they are also variationally correct. This is not so simple in a general quadrilateral where the complication arising from the isoparametric mapping from a natural co-ordinate system to a Cartesian system makes it very difficult to see the consistent form clearly. We shall see the difficulties associated with this form in a later section.

6.3.2 The quadratic 8-node and 9-node plate elements

The 4-node plate element described above is based on bi-linear functions. It would seem that an higher order element based on quadratic functions would be far more accurate. There are now two possibilities, an 8-node element based on what are called the serendipity functions and a 9-node element based on the Lagrangian bi-quadratic functions. There has been a protracted debate on which version is more useful, both versions having fiercely committed protagonists. By now, it is well known that the 9-node element in its rectangular form is free of shear locking even with exact integration of shear energy terms and that its performance is vastly improved when its shear strain energies are integrated in a selective sense (2×3 and 3×2 rules for γ_{xz} and γ_{yz} terms respectively). It is in fact analogous to the quadratic Timoshenko beam element, the field-inconsistencies not being severe enough to cause locking. This is however not true for the 8-node element which was derived from the Ahmad shell element [6.3] and which actually pre-dates the 4-node Mindlin element. An exact integration of bending and shear strain energies resulted in an element that locked for most practical boundary suppressions even in its rectangular form. Many ad-hoc techniques e.g. the reduced and selective integration techniques, hybrid and mixed methods, etc. failed or succeeded only partially. It was therefore regarded for some time as an unreliable element as no quadrature rule seemed to be able to eliminate locking entirely without introducing other deficiencies. It seems possible to attribute this noticeable difference in the performance of the 8- and 9-node elements to the missing central node in the former. This makes it more difficult to restore consistency in a simple manner.

6.3.3 Stress recovery from Mindlin plate elements

The most important information a structural analyst looks for in a typical finite element static analysis is the state of stress in the structure. It is therefore very important for one to know points of optimal stresses in the Mindlin plate elements. It is known that the stress recovery at nodes from displacement elements is unreliable, as the nodes are usually the points where the strains and stresses are least accurate. It is possible however to determine points of optimal stress recovery using an interpretation of the displacement method as a procedure that obtains strains over the finite element domain in a least-squares accurate sense. In Chapter 2, we saw a basis for this interpretation. We can apply this rule to determine points of accurate stress

recovery in the Mindlin plate elements. For a field-consistent rectangular 4-node element, the points are very easy to determine [6.8] (note that in a field-inconsistent 4-node element, there will be violent linear oscillations in the shear stress resultants corresponding to the inconsistent terms). Thus, Ref. 6.8 shows that bending moments and shear stress resultants Q_{xz} and Q_{yz} are accurate at the centroid and at the 1×2 and 2×1 Gauss points in a rectangular element for isotropic or orthotropic material. It is coincidental, and therefore fortuitous, that the shear stress resultants are most accurate at the same points at which they must be sampled in a selective integration strategy to remove the field-inconsistencies! For anisotropic cases, it is safest to sample all stress resultants (bending and shear) at the centroid.

Such rules can be extended directly to the 9-node rectangular element. The bending moments are now accurate at the 2×2 Gauss points and the shear stress resultants in an isotropic or orthotropic problem are optimal at the same 2×3 and 3×2 Gauss points which were used to remove the inconsistencies from the strain definitions. However, accurate recovery of stresses from the 8-node element is still a very challenging task because of the difficulty in formulating a robust element. The most efficient elements known today are variationally incorrect even after being made field-consistent and need special filtering techniques before the shear stress resultants can be reliably sampled.

So far, discussion on stress sampling has been confined to rectangular elements. When the elements are distorted, it is no simple matter to determine the optimal points for stress recovery - the stress analyst must then exercise care in applying these rules to seek reliable points for recovering stresses.

6.4 Concluding remarks

We can conclude this section on *shear locking* by noting that the available understanding was unable to resolve the phenomena convincingly. The proposed improvement, which was the consistency paradigm, together with the functional re-constitution procedure, allowed us to derive an error estimate for a case under locking and we could show through numerical (digital) experiments that these estimates were accurate. In this way we are convinced that a theory with the consistency paradigm is more successful from the falsifiability point of view than one without.

6.5 References

6.1 G. Prathap and C. R. Babu, Field-consistent strain interpolations for the quadratic shear flexible beam element, *Int. J. Num. Meth. Engng.* 23, 1973-1984, 1986.

6.2 R. D. Mindlin, Influence of rotary inertia and shear on flexural motion of elastic plates, *J. Appl. Mech.* 18, 31-38, 1951.

6.3 S. Ahmad, B. M. Irons and O. C. Zienkiewicz, Analysis of thick and thin shell structures by curved finite elements, *Int. J. Num. Meth. Engng.* 2, 419-451, 1970.

6.4 T. J. R. Hughes, R. L. Taylor and W. Kanoknukulchal, A simple and efficient finite element for plate bending, *Int. J. Num. Meth. Engng.* 411, 1529-1543, 1977.

6.5 S. F. Pawsey and R. W. Clough, Improved numerical integration of thick shell finite elements, *Int. J. Num. Meth. Engng.* 43, 575-586, 1971.

6.6 O. C. Zienkiewicz, R. L. Taylor and J. M. Too, Reduced integration technique in general analysis of plates and shells, *Int. J. Num. Meth. Engng.* 43, 275-290, 1971.
6.7 H. Stolarski and T. Belytschko, Membrane locking and reduced ingression for curved elements, *J. Appl. Mech.* 49, 172-178, 1982.
6.8 G. Prathap and C. R. Babu, Accurate force evaluation with a simple bi-linear plate bending element, *Comp. Struct.* 25, 259-270, 1987.